

Multifrequency signal generation in a magnonic ring autooscillator based on a superthin yttriumirongarnet film

© A.S. Bir¹, D.V. Romanenko¹, S.V. Grishin¹, S.A. Nikitov^{1,2}

¹ Saratov National Research State University, Saratov, Russia

² Kotelnikov Institute of Radio Engineering and Electronics, Russian Academy of Sciences, Moscow, Russia

E-mail: sergrsh@yandex.ru

Received September 11, 2024

Revised November 14, 2024

Accepted November 14, 2024

The paper presents the results of an experimental study of generation modes of a multifrequency microwave (MW) signal in a ring autooscillator with a magnonic crystal (MC) based on a submicronthick yttriumirongarnet film. It has been established that generation of the multifrequency MW signal takes place when MC operates in the nonlinear mode. The signal is formed on both sides of the frequency of the crystal's first bandgap belonging to the magnetostatic surface spinwave band. The possibility of controlling the spectrum of the multifrequency MW signal by varying the external direct magnetic field has been demonstrated.

Keywords: spin waves, magnonic crystal, YIG-oscillator.

DOI: 10.61011/TPL.2025.03.60726.20114

In magnonics, one of the important fields is studying the propagation and interaction of spin waves (SW) in superthin yttriumirongarnet (YIG) films [1–3]. First of all, this is associated with the desire to miniaturize spinwave devices and transfer them to the nanometer scale. In addition, in superthin YIG films $d \leq 2 \cdot 10^{-7}$ m thick adjacent to superthin layers of normal metal (e.g. platinum) there arise effects associated either with the influence of spinpolarized current on the SW losses [4,5] or with EMF induction by SW [6–8]. In the first case, the SW attenuation/enhancement by the spinpolarized current occurs due to the direct spin Hall effect in a normal metal; in the second case, the EMF induction in the normal metal is caused by the inverse spin Hall effect.

At present, there are three known techniques for creating superthin YIG films having thicknesses from units to hundreds of nanometers. The first of them is based on using the liquidphase epitaxy method [3,4,6] which was widely used previously to grow micronthick YIG films on gadoliniumgalliumgarnet (GGG) substrates. The second technique employs the pulsed laser deposition method [7,9,10], while the third one is based on the method of magnetron sputter deposition of superthin YIG films on GGG substrates [11,12]. Depending on the method selected, the Gilbert attenuation constant varies from 10^{-4} to 10^{-3} and is not inferior to similar values obtained for the micronthick YIG films. A specific feature of superthin YIG films is that, using submicron— and nanometerwide excitation antennas ($w \sim d$, where w is the excitation antenna width), it is possible to excite in them SWs with longitudinal wave numbers k much higher than in micronthick YIG films where SWs are excited by antennas about tens of micrometers in width. As a consequence, SWs excited in superthin YIG films by antennas of smaller width

have lower group velocities V_g than those in micronthick YIG films. This decreases the SW propagation length to $l \sim (10–100) \cdot 10^{-6}$ m which is much shorter than that in micronthick YIG films ($l \sim 10^{-2}$ m).

Theoretical study [13] has demonstrated the possibility of using a delay line based on the superthin YIG film in the feedback circuit of active ring resonator. In this study, we have calculated the spectrum of eigenmodes of the active ring resonator in the pregeneration mode and shown the multifrequency spectrum rearrangement (the frequency interval between adjacent modes is defined as $\Delta f = V_g(f)/l$ and is almost constant) with varying YIG film thickness and SW propagation length. We have revealed that frequency interval Δf for the superthin YIG film with $d = 10^{-7}$ m and $l = 56 \cdot 10^{-6}$ m is 6.9 MHz at the frequencies of about 5 GHz.

To control the spectrum of the active ring resonator eigenmodes, a magnonic crystal (MC) is also used, which is, e.g. a YIG film periodically modulated across the thickness [14–17]. It participates in controlling the ringmode resonant frequencies [14], in forming both a monochromatic signal with low phase noise [15] and chaotic microwave signal in the form of a sequences of various (light or dark) dissipative envelope solitons [16,17].

In this work, we have demonstrated experimentally the possibility of generating a multifrequency microwave signal in a ring autooscillator involving MC created based on a superthin YIG film.

The magnon ring autooscillator is schematically represented in Fig. 1. Such a ring oscillator consists of a solidstate microwave amplifier based on GaN transistors. The amplifier's gain is 55 dB in the frequency band of 2–8 GHz. It operates in the mode of linear microwave signal amplification, and its only function is to compensate

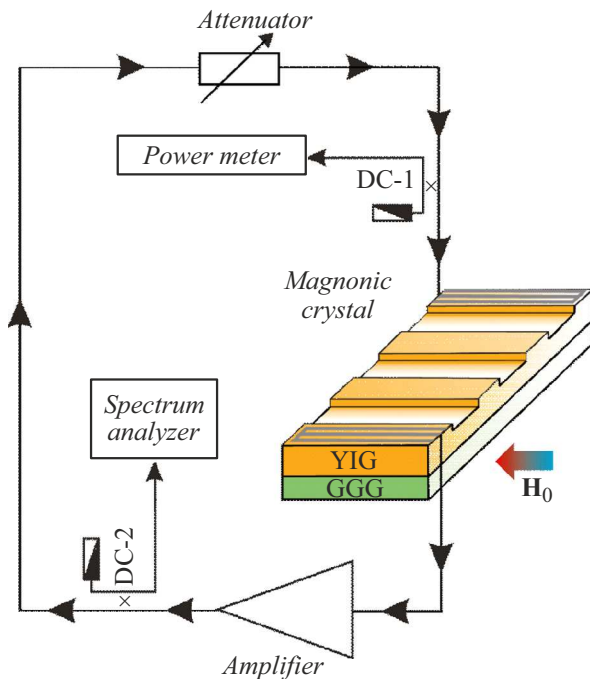


Figure 1. Schematic representation of a magnon ring auto-oscillator based on the delay line with MC.

the MW signal loss in the ring. The signal is fed from the MW amplifier output to the variable attenuator input and, further, to the input of the MC-based delay line; after that, it again comes to the MW amplifier input. The variable attenuator controls the signal power level at the input of delay line that is, in general, a nonlinear element. Most of the MW signal power is returned from the MW amplifier output back to the ring; its smaller part is fed to the input of spectrum analyzer E4408B.

The delay line consists of two (input and output) coplanar MW antennas formed on the YIG waveguide surface by optical lithography with metal masks. The metal masks were applied by using a magnetron sputtering unit. Each coplanar MW antenna consists of two lateral (grounded) and one central (signal) strips $w_s = 2.4 \mu\text{m}$ wide. One end of each strip is connected to a load (oscillator or receiver), while the other is connected to the other two strips. The distance between the lateral and central strips is $w_g = 2 \mu\text{m}$; the length of all three strips of each antenna is $L_{\text{CPL}} = 70 \mu\text{m}$. The input MW antenna converts the MW signal supplied to it into a spin wave (SW), while the output MW antenna converts SW back into MW signal. Distance between the central strips of two coplanar transmission lines is $L_d = 50 \mu\text{m}$.

The YIG film grown by liquid-phase epitaxy on the GGG substrate has the thickness of $d = 10^{-7}$ m, effective YIG film near-surface magnetization of $4\pi M_{\text{eff}} \cong 0.175$ T, and ferromagnetic resonance line width of $2\Delta H \cong 87.535$ A/m at the frequencies of ~ 3 GHz. The YIG waveguide is characterized by the width of $W = 50 \mu\text{m}$ and length of $L = 500 \mu\text{m}$. To create a YIG waveguide with a periodically

modulated thickness (magnon crystal), ion etching of the YIG film was used, which was carried out on an ion-beam etching setup with vacuum universal post VUP-5. The etching depth was 10 nm (10% of the YIG waveguide thickness), the etched section (groove) width was $2 \mu\text{m}$, and structure period T was $4 \mu\text{m}$. Distance L_d between the antennas accommodates nine MC periods. External direct magnetic field \mathbf{H}_0 is applied tangentially to the YIG waveguide surface and is directed along the coplanar MW antennas. This field orientation allows exciting in the YIG waveguide a surface magnetostatic spin wave (SMSW).

Fig. 2 presents the amplitude-frequency response (AFR) of the delay line based on a superthin YIG film having one-dimensional periodic structure. The delay line AFR was measured outside the oscillator circuit using a vector network analyzer for magnetic field $H_{01} = 34.22$ kA/m. Evidently, here the minimum level of loss is 52–55 dB which is significantly higher than that previously observed in the delay line with the micron-thick YIG film because of a higher $2\Delta H$. In addition, the SMSW spectrum has a well-pronounced dip with the maximum level of MW signal attenuation of about 95 dB at the frequency of $f_{01} = 2785$ MHz. On either side of this dip, two (left and right) passbands get formed; a multifrequency MW signal will subsequently be formed in each of them.

Fig. 2, *b* presents the SMSW dispersion characteristic constructed based on the measured phase-frequency characteristic of the MC-based delay line. In constructing this dependence, the SMSW wave numbers k were defined as $k = \Delta\varphi/L_d$, where $\Delta\varphi$ is the „unwrapped“ phase increment in the MC-based delay line. From the obtained SMSW dispersion characteristic exhibits at frequency f_{01} a discontinuity corresponding to the SMSW wave number $k_{b1} = 7.1 \cdot 10^5$ rad/m. The obtained SMSW wave number practically coincides with that of the MC first bandgap determined from the Bragg condition as $k_{b1} = \pi/T = 7.85 \cdot 10^5$ rad/m. Thus, this dip in the MC-based delay line AFR is the first bandgap of MC.

Fig. 3, *a* demonstrates a power spectrum of the multifrequency MW signal generated in the ring oscillator with the MC-based delay line at $H_{01} = 34.22$ kA/m. One can see that the multifrequency MW signal is generated on both sides of the MC first bandgap frequency and possesses a virtually equidistant spectrum. The multifrequency MW-signal spectrum section located to the left of frequency f_{01} is characterized by average frequency offset $\Delta f_{lb1} = 7.9$ MHz between the signal's spectral components. Another signal spectrum section located to the right of frequency f_{01} is characterized by average frequency offset $\Delta f_{rb1} = 7.4$ MHz. Both frequency offsets are directly proportional to the SMSW group velocity which, as the obtained results show, varies in the delay line frequency band by less than 10%.

Note that in our case the MW signal generation is immediately multifrequency and becomes observable when the nonlinear threshold is exceeded by about 10 dB. At the selected magnetic field, to the nonlinear threshold the signal power level at the delay line input corresponds, which is

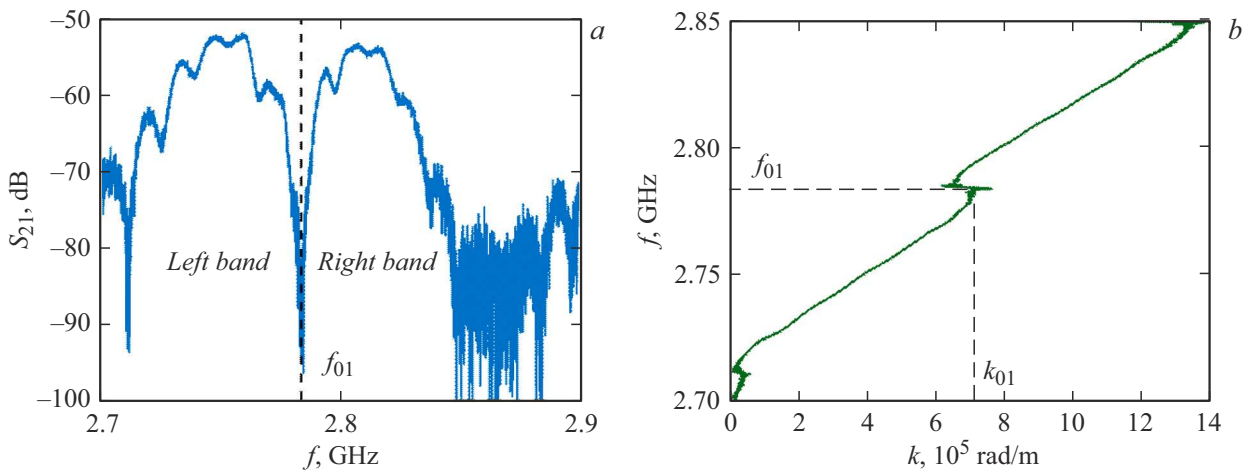


Figure 2. Amplitude-frequency response of the MCbased delay line (a) and frequency dependence on the SMSW wave number (b). Measurements on both fragments were performed at $H_{01} = 34.22$ kA/m and power of the monochromatic MW signal at the delay line input of -30 dBm.

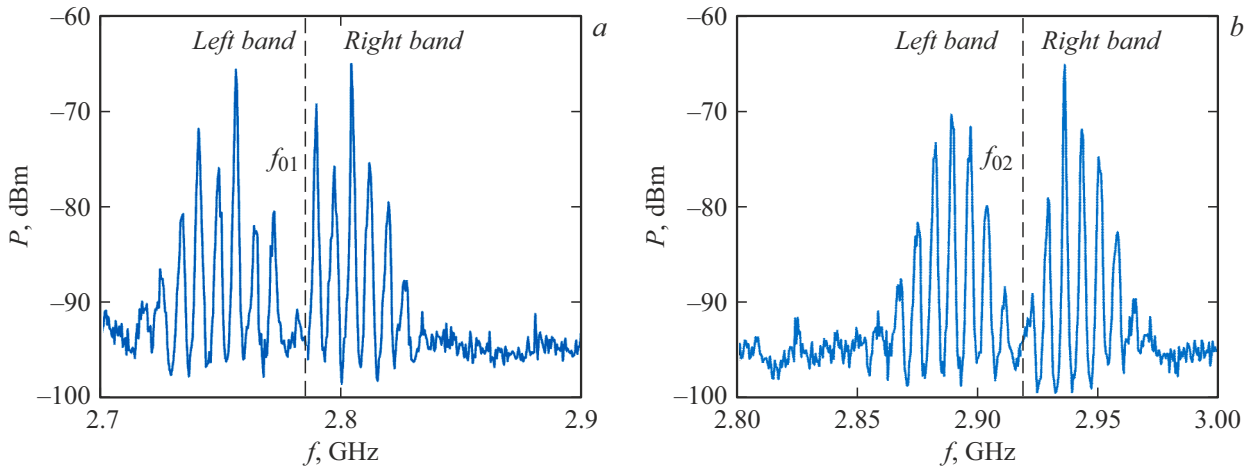


Figure 3. Power spectra of the multifrequency MW signal generated in the MCbased magnon ring autooscillator at $H_{01} = 34.22$ kA/m (a) and $H_{02} = 37.96$ kA/m (b). Power of the multifrequency MW signal at the input of the MCbased delay line is -15 (a) and -14.5 dBm (b).

about $50 \mu\text{W}$. Such relatively low signal power levels are characteristic of nonlinear parametric threewave processes of the SMSW decay which, as shown in [18], cannot be observed in superthin YIG films less than 200 nm thick. However, as per [19], in YIG films there always exists a so-called transition layer between the YIG film and GGG substrate, whose magnetization differs from that of the film itself and drops to zero near the GGG substrate surface. The transition layer is about 200 nm thick, and its influence becomes significant after transferring from micronthick YIG films to superthin submicron— and nanometerthick YIG films. Thus, SMSW excited by a coplanar antenna near the surface of the YIG film with the effective magnetization of about 0.175 T can in turn parametrically excite dipole-exchange SWs only in the immediate vicinity of the GGG substrate surface where the magnetization has a value at which the excited SW frequencies amount to a half of the SMSW frequency. Just the presence of the transition layer

or a magnetization gradient across the YIG film thickness are the main reasons for the existence in the superthin YIG film 100 nm thick of a nonlinear threewave parametric decay of SMSW.

Fig. 3, b demonstrates the possibility of controlling the spectrum of the generated multifrequency MW signal by varying the magnetic field strength. It is evident that an increase in the field strength to $H_{02} = 37.96$ kA/m leads to an increase in the frequency of the MC first bandgap ($f_{02} = 2919$ MHz) and to the signal spectrum rearrangement upward in frequency. Thereat, reduction in frequency offsets is observed both to the left ($\Delta f_{lb2} = 7.3$ MHz) and to the right ($\Delta f_{rb2} = 6.9$ MHz) of frequency f_{02} . This fact indicates a decrease in the SMSW group velocity with increasing magnetic field strength, which is consistent with the known results for micronthick YIG films.

In conclusion, note that the experimental results obtained in this study indicate the necessity of taking into account

nonlinear threewave parametric processes of magnetostatic SW decay in superthin YIG films in creating models of microminiature MW generators [13] and other devices based on such films [20–22] operating at frequencies below 4.9 GHz.

Funding

The study was supported by the Russian Science Foundation (project № 23-79-30027).

Conflict of interests

The authors declare that they have no conflict of interests.

References

- [1] Q. Wang, G. Csaba, R. Verba, A.V. Chumak, P. Pirro, *Phys. Rev. Appl.*, **21** (4), 040503 (2024). DOI: 10.1103/PhysRevApplied.21.040503
- [2] J. Xu, C. Zhong, S. Zhuang, C. Qian, Y. Jiang, A. Pishchvar, X. Han, D. Jin, J.M. Jornet, B. Zhen, J. Hu, L. Jiang, X. Zhang, *Phys. Rev. Lett.*, **132** (11), 116701 (2024). DOI: 10.1103/PhysRevLett.132.116701
- [3] C. Dubs, O. Surzhenko, R. Thomas, J. Osten, T. Schneider, K. Lenz, J. Grenzer, R. Hübner, E. Wendler, *Phys. Rev. Mater.*, **4** (2), 024416 (2020). DOI: 10.1103/PhysRevMaterials.4.024416
- [4] M. Evelt, V.E. Demidov, V. Bessonov, S.O. Demokritov, J.L. Prieto, M. Muñoz, J. Ben Youssef, V.V. Naletov, G. de Loubens, O. Klein, M. Collet, K. Garcia-Hernandez, P. Bortolotti, V. Cros, A. Anane, *Appl. Phys. Lett.*, **108** (17), 172406 (2016). DOI: 10.1063/1.4948252
- [5] M. Collet, X. de Milly, O. d'Allivy Kelly, V.V. Naletov, R. Bernard, P. Bortolotti, J. Ben Youssef, V.E. Demidov, S.O. Demokritov, J.L. Prieto, M. Muñoz, V. Cros, A. Anane, G. de Loubens, O. Klein, *Nat. Commun.*, **7**, 10377 (2016). DOI: 10.1038/ncomms10377
- [6] V. Castel, N. Vlietstra, J. Ben Youssef, B.J. van Wees, *Appl. Phys. Lett.*, **101** (13), 132414 (2012). DOI: 10.1063/1.4754837
- [7] O. d'Allivy Kelly, A. Anane, R. Bernard, J. Ben Youssef, C. Hahn, A.H. Molpeceres, C. Carrétéro, E. Jacquet, C. Deranlot, P. Bortolotti, R. Lebourgeois, J.-C. Mage, G. de Loubens, O. Klein, V. Cros, A. Fert, *Appl. Phys. Lett.*, **103** (8), 082408 (2013). DOI: 10.1063/1.4819157
- [8] M.E. Seleznev, Yu.V. Nikulin, V.K. Sakharov, Yu.V. Khivintsev, A.V. Kozhevnikov, S.L. Vysotskiy, Yu.A. Filimonov, *ZhTF*, **91** (10), 1504 (2021). (in Russian) DOI: 10.61011/TPL.2025.03.60726.20114 M.E. Seleznev, Yu.V. Nikulin, V.K. Sakharov, Yu.V. Khivintsev, A.V. Kozhevnikov, S.L. Vysotskiy, Yu.A. Filimonov, *Tech. Phys.*, **67** (13), 2074 (2022). DOI: 10.61011/TPL.2025.03.60726.20114
- [9] A.K. Kaveev, V.E. Bursian, S.V. Gastev, B.B. Krichevstov, S.M. Suturin, M.P. Volkov, N.S. Sokolov, *Tech. Phys. Lett.*, **42** (12), 1156 (2016). DOI: 10.1134/S1063785016120075
- [10] B.B. Krichevstov, A.M. Korovin, S.M. Suturin, A.V. Telegin, I.D. Lobov, N.S. Sokolov, *Thin Solid Films*, **756**, 139346 (2022). DOI: 10.1016/j.tsf.2022.139346
- [11] T. Liu, H. Chang, V. Vlaminck, Y. Sun, M. Kabatek, A. Hoffmann, L. Deng, M. Wu, *J. Appl. Phys.*, **115** (17), 17A501(2014). DOI: 10.1063/1.4852135
- [12] H. Chang, P. Li, W. Zhang, T. Liu, A. Hoffmann, L. Deng, M. Wu, *IEEE Magn. Lett.*, **5**, 6700104 (2014). DOI: 10.1109/LMAG.2014.2350958
- [13] A.A. Nikitin, I.Yu. Tatsenko, M.P. Kostylev, A.B. Ustinov, *J. Appl. Phys.*, **135** (12), 123906 (2024). DOI: 10.1063/5.0200249
- [14] A.V. Bagautdinov, A.B. Ustinov, *Tech. Phys. Lett.*, **49** (7), 12 (2023). DOI: 10.61011/TPL.2025.03.60726.20114
- [15] E. Bankowski, T. Meitzler, R.S. Khymyn, V.S. Tiberkevich, A.N. Slavin, H.X. Tang, *Appl. Phys. Lett.*, **107** (12), 122409 (2015). DOI: 10.1063/1.4931758
- [16] S.V. Grishin, Yu.P. Sharaevskii, S.A. Nikitov, E.N. Beginin, S.E. Sheshukova, *IEEE Trans. Magn.*, **47** (10), 3716 (2011). DOI: 10.1109/TMAG.2011.2158293
- [17] A.S. Bir, S.V. Grishin, A.A. Grachev, O.I. Moskalenko, A.N. Pavlov, D.V. Romanenko, V.N. Skorokhodov, S.A. Nikitov, *Phys. Rev. Appl.*, **21** (4), 044008 (2024). DOI: 10.1103/PhysRevApplied.21.044008
- [18] V. Castel, N. Vlietstra, B.J. van Wees, *Phys. Rev. B*, **90** (21), 214434 (2014). DOI: 10.1103/PhysRevB.90.214434
- [19] V.V. Tikhonov, V.A. Gubanov, S.A. Nikitov, A.V. Sadovnikov, *J. Magn. Magn. Mater.*, **562**, 169763 (2022). DOI: 10.1016/j.jmmm.2022.169763
- [20] S. Watt, M. Kostylev, *Phys. Rev. Appl.*, **13** (3), 034057 (2020). DOI: 10.1103/PhysRevApplied.13.034057
- [21] A.B. Ustinov, R.V. Haponchyk, M. Kostylev, *Appl. Phys. Lett.*, **124** (4), 042405 (2024). DOI: 10.1063/5.0189542
- [22] A.A. Nikitin, R.V. Haponchyk, I.Yu. Tatsenko, M.P. Kostylev, A.B. Ustinov, *Tech. Phys.*, **69** (11), 1736 (2024).

Translated by EgoTranslating